PAPER

NJC

www.rsc.org/njc

Solid state study of the copper(II) complex of 2-hydroxyiminopropanoic acid†

Kamilla Malek,[ab] Martin Vala,[b] Jolanta Swiatek-Kozlowska[c] and Leonard M. Proniewicz[ad]

[a] *Faculty of Chemistry, Jagiellonian University, ul. Ingardena 3, 30-060, Krakow, Poland. E-mail: proniewi@chemia.uj.edu.pl; Fax: +48 12 634 05 15; Tel: +48 12 633 63 77 ext. 2253*
[b] *Department of Chemistry and Center for Chemical Physics, University of Florida, Gainesville, FL 32611-7200, USA*
[c] *Department of Basic Medical Sciences, Medical University of Wroclaw, ul. J. Kochanowskiego 14, 51-601, Wroclaw, Poland*
[d] *Regional Laboratory of Physicochemical Analysis and Structural Research, Jagiellonian University, ul. Ingardena 3, 30-060, Krakow, Poland*

Received* (in Toulouse, France) *11th June 2003, Accepted 30th October 2003
First published as an Advance Article on the web 27th February 2004

A copper(II) complex of 2-hydroxyiminopropanoic acid (hpa) has been prepared and characterized by X-ray analysis, infrared, Raman and EPR spectra. The bidentate hpa ligand chelates the copper ion through the oxime nitrogen and the carboxyl oxygen to form an anionic bis-complex. An intramolecular H-bond stabilizes the two ligands in a cis planar coordination. Equilibrium geometries, harmonic vibrational frequencies, infrared and Raman intensities were calculated for hpa and its copper(II) complex by using DFT (B3LYP) and Hartree–Fock methods with 6-31G(d) and Lanl2DZ basis sets. The computed properties are compared to the experimental values.

Introduction

The 2-hydroxyiminopropanoic acid (hpa) ligand is similar to α-alanine, but with the alanine amino group ($CH–NH_2$) replaced by the hpa oxime moiety (C=NOH). As with amino acids, oximes have been widely studied as a class and have shown some medical and biological functions, such as agents in the treatment of rheumatoid arthritis,[1] prostate cancer,[2] malaria,[3] Alzheimer's disease and AIDS related dementia,[4] chemical warfare poisoning[5] or in the biosynthesis of nitrogen oxide.[6] Although a pharmaceutical function of the title oxime has not yet been shown, interest in hpa is increasing in connection with its chelating ability with transition metal ions. Structural modification of the amino group can lead to considerable variation in coordination properties and specificity. The coordinating ability of oxime analogs of amino acids with nickel(II) and copper(II) ions has been investigated extensively in solution.[7–10] Oximes have a strong tendency to form bis-chelate square planar structures. Cis/trans complex formation depends critically on the substituents adjacent to the α-carbon, as well as on the number of other available binding sites.

In this work, we present a study of the hpa copper(II) complex in the solid state. We report X-ray crystallographic evidence for monomeric complex formation and vibrational spectra in the far- and mid-infrared (IR) regions of the ligand and complex. We also present electronic paramagnetic resonance measurements of the complex. The infrared and Raman frequencies and intensities of the vibrational modes for hpa and its copper complex were computed at the HF/6-31G(d) and B3LYP/Lanl2DZ levels of theory, respectively. To give a detailed description of the calculated and observed vibrational modes, normal coordinate analysis calculations (PED, Potential Energy Distribution) of the ligand and the complex were also performed.

Experimental

Preparations

Hpa (L). 2-Hydroxyiminopropanoic acid was synthesized according to the literature method.[11–13] Elemental analysis (C, H, N) was conducted at the Faculty of Chemistry of Jagiellonian University according to standard microanalytical procedures (found: C, 35.1; H, 4.8; N, 13.4; calcd For $C_3H_5NO_3$: C, 34.9; H, 4.9; N, 13.6%).

$K[CuHL_2]\cdot H_2O$. An aqueous solution of $Cu(NO_3)_2\cdot 2.5H_2O$ (56.7 mg in 5 ml H_2O, 0.24 mmol) was added to hpa (50 mg, 0.48 mmol) dissolved in water (5 ml) with stirring. The turbid blue solution was stirred (20 min) and treated dropwise with 1 M KOH (to pH 5). The resulting clear dark blue solution was heated and stirred (1 h), and then filtered and concentrated by evaporation at room temperature. Black-violet crystals began to form within a week. Due to co-precipitation of the complex and KNO_3, elemental analysis could not be performed. In the polycrystalline sample, the metal-to-ligand molar ratio (1:2) was confirmed by a standard analytical procedure (AAS).

Crystallography‡

Crystal data and other experimental details are presented in Table 1. Data were collected at 173 K on a Siemens SMART Platform equipped with a CCD area detector and a graphite

† Electronic supplementary information (ESI) available: bond lengths, bond angles and hydrogen bonds for $K[CuHL_2]\cdot H_2O$; harmonic frequencies, IR and Raman intensities and potential energy distributions for hpa and $K[CuHL_2]\cdot H_2O$. See http://www.rsc.org/suppdata/nj/b3/b307066m/

‡ CCDC reference numbers 228299. See http://www.rsc.org/suppdata/nj/b3/b307066m/ for crystallographic data in .cif or other electronic format.

DOI: 10.1039/b307066m

Table 1 Crystal data and structure refinement details for $K[CuHL_2]\cdot H_2O$

Empirical formula	$C_6H_9CuKN_2O_7$
Formula weight	323.79
Temperature/K	193(2)
Wavelength/Å	0.71073
Crystal system	Triclinic
Space group	*P*-1
a/Å	8.6072(7)
b/Å	11.550(2)
c/Å	11.857(2)
α/°	99.737(2)
β/°	92.727(2)
γ/°	109.999(2)
U/Å^3	1084.7(2)
Z	4
μ/mm^{-1}	2.423
Total reflections	6978
Indep. reflections	4738
R(int)	0.0606
Obs. reflections [$I > 2\sigma(I)$]	3562
$R_1{}^a$ [$I > 2\sigma(I)$]	0.0333
$wR_2{}^b$ [$I > 2\sigma(I)$]	0.0836
$R_1{}^a$ (all data)	0.0507
$wR_2{}^b$ (all data)	0.0893

^{a} $R_1 = \sum(||F_o| - |F_c||)/\sum|F_o|$ ^{b} $wR_2 = [\sum[w(F_o^2 - F_c^2)^2]/\sum[w(F_o^2)^2]]^{1/2}$; weighting scheme applied: $w = 1/[\sigma^2(F_o^2) + (0.0456p)^2 + 0.0p]$, where $p = [\max(F_o^2, 0) + 2F_c^2]/3$.

monochromator utilizing MoK_α radiation ($\lambda = 0.71073$ Å) at the University of Florida. Cell parameters were refined using up to 8192 reflections. A full sphere of data (1381 frames) was collected using the ω-scan method (0.3° frame width). The first 50 frames were remeasured at the end of data collection to monitor instrument and crystal stability (maximum correction on *I* was <1%). Absorption corrections by integration were applied based on measured indexed crystal faces.

The structure was solved by direct methods in SHELXTL5[14] and refined using full-matrix least-squares method. The non-H atoms were treated anisotropically, whereas the hydrogen atoms were calculated in ideal positions and assumed to be attached to their respective carbon atoms, except for H3, H9 and the water H atoms, which were obtained from a difference Fourier map and refined without any constraints. H3 and H9 are located midway between O3 and O4, and O9 and O10, respectively. The asymmetric unit consists of two complexes and two water molecules. A total of 336 parameters were refined in the final cycle of refinement using 3562 reflections with $I > 2\sigma(I)$ to yield R_1 and wR_2 of 3.33% and 8.36%, respectively. Refinement was done using F^2.

Spectroscopic measurements

For FT-Raman measurements, a few milligrams of hpa and $K[CuHL_2]\cdot H_2O$ were measured in capillary tubes directly; 512 and 3000 scans were collected (with a resolution of 4 cm^{-1}) for hpa and its complex, respectively. Fourier transform mid-infrared (FT-MIR, 256 scans) and Fourier transform far-infrared (FT-FIR, 512 scans) spectra were obtained on CsI and low molecular weight polyethylene discs, respectively. Resolution was 4 cm^{-1} (MIR) and 2 cm^{-1} (FIR). FT-Raman spectra were recorded on a Bio-Rad step-scan spectrometer (FTS 6000) combined with a Bio-Rad Raman accessory (FTS 40). Excitation at 1064 nm was effected by a Spectra Physics Topaz T10-106c cw Nd:YAG laser. FT-IR spectra were measured on Bruker (IFS 48) and Bio-Rad (FTS 60 V) spectrometers in the mid- and far-IR regions, respectively. Frequency accuracy is estimated as ±1 cm^{-1}.

The ESR spectra of $K[CuHL_2]\cdot H_2O$ were recorded on a Bruker spectrometer [ELEX SYS X500, X-band (9.5 GHz)] at 77 and 298 K. Also the temperature dependence of the ESR spectra was determined over the temperature range 100 to 340 K.

Computational procedures

Ab initio (RHF) and DFT (B3LYP)[15,16] calculations with 6-31G(d) and Lanl2DZ[17,18] basis sets (for the ligand and the complex, respectively) were performed using the Gaussian 98 program.[19] Optimum geometries and harmonic frequencies were determined on an SGI 2800 computer in the Academic Computer Center "Cyfronet" in Krakow. The potential energy distributions (PED) were obtained using the Veda program.[20]

Results and discussion

Crystal structure of the copper(II)–2-(hydroxyimino)propanoic acid complex

A perspective view of the copper(II)–2-(hydroxyimino)propanoic acid complex is shown in Fig. 1. Selected bond lengths and angles are given in the Electronic supplementary information (ESI, Tables I and II). The complex consists of the anion, $[CuHL_2]^-$, the counter ion, K^+, and several water molecules hydrogen-bonded to the anion. The X-ray measurement showed the presence of a pair of crystallographically distinct, chemically equivalent complexes. In the crystal packing (Fig. 2), the complex anions align as chains along the *y* direction. The intrachain copper–copper distance is 8.878 Å, while the interplanar Cu–Cu distance is 4.248 Å. The copper(II) ion coordination is approximately square planar, formed by the two nitrogens of the oximic groups and the two oxygens of the carboxyl groups. Two molecules of hpa chelate to the metal atom in cis fashion, forming five-membered rings. They are bonded by intramolecular hydrogen bonds between the two oxime oxygens. The crystal structure of the Cu^{2+}–hpa complex agrees well with the structure proposed from solution potentiometric studies.[7] The Cu–N bond distances for both complex anions are in the range 1.935–1.945 Å, comparable to those in related complexes.[21–26] The Cu_1N_1 and Cu_1N_2 distances are almost equal [1.945(2), 1.943(2) Å], whereas the Cu_2N_3 distance (1.935 Å) is shorter than the Cu_2N_4 distance by 0.009 Å, because of a more asymmetric hydrogen bond. The Cu–O distances are almost the same in both molecules. However, the first exhibits a more symmetrical coordination

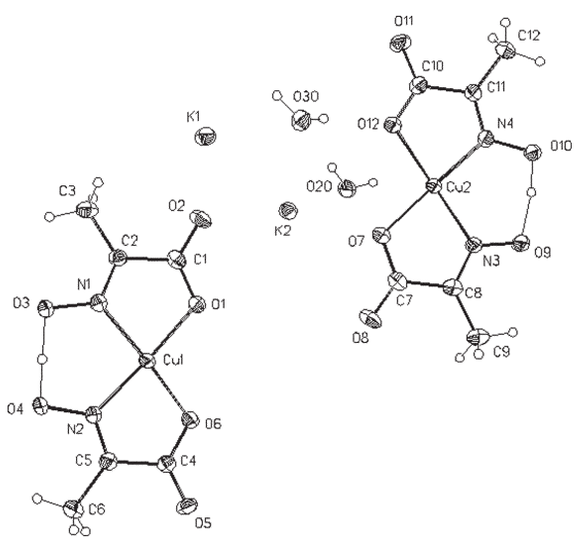

Fig. 1 Crystal structure and numbering scheme of $K[CuHL_2]\cdot H_2O$.

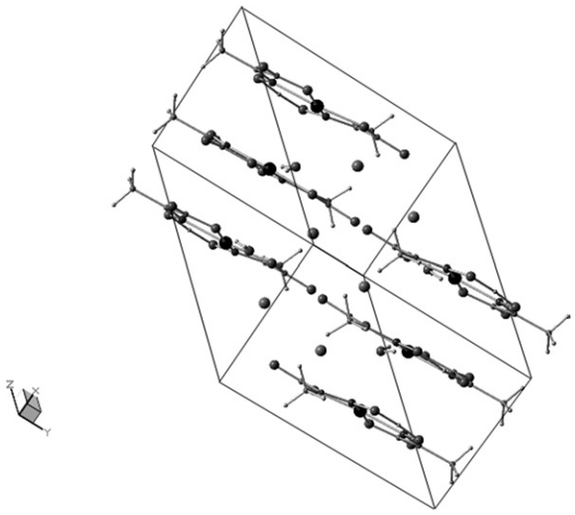

Fig. 2 Packing of molecules of the copper(II)-2-hydroxyiminopropanoic complex.

around the copper atom. The carbonyl bond lengths in the complex lengthen slightly (0.02 Å) after coordination, whereas the C–O bonds chelating to the copper ion shorten considerably (0.03 Å).[27] The C=N and N–O distances are quite different due to the deprotonation of the oximic group. The C=N bond distance becomes longer (1.29 Å), whereas the N–O bond becomes shorter (1.35 Å). After chelation, the CNO angle opens by ~8° (from 112.8° in hpa). The intramolecular hydrogen-bridged O–H···O$^-$ distance is ~2.47 Å, a value that is typical for many square-planar cis oximic complexes.[21,22,24,25,28,29]

ESR properties of the copper(II)–2-(hydroxyimino)propanoic acid complex

The X-band EPR spectrum of a polycrystalline sample of the hpa complex is shown in Fig. 3. The 298 K spectrum shows a single, slightly anisotropic signal, with no hyperfine splitting, centered at $g = 2.097$, which is close to the spin-only value of 2.002. Cooled to 77 K, the spectrum is almost identical, with a g value of 2.093, confirming that the geometry of the ligand around the Cu(II) ion is unchanged. However, in ethane–1,2-diol–water solution (120 K), hyperfine structure was observed ($g_{\|} = 2.230$, $A_{\|} = 185 \times 10^4 T$).[7] The coordination in solution is thus the same as in our case (*viz.* in the solid).[7] The ESR behavior of the present complex is most likely caused by spin-exchange between paramagnetic copper centers. EPR studies of such exchange-coupled transition metal systems have been reported extensively in the past, but mainly for ligand-bridged complexes.[26,28,30–35] The present crystallographic data shows that the $K[CuHL_2]\cdot H_2O$ solid consists of intercomplex dimers (Cu–Cu, 4.248 Å) and colinear intercomplex dimers (Cu–Cu, 8.878 Å). From these Cu–Cu distances, it might be expected that the predominant spin-spin interaction should occur between the closer lying coppers.

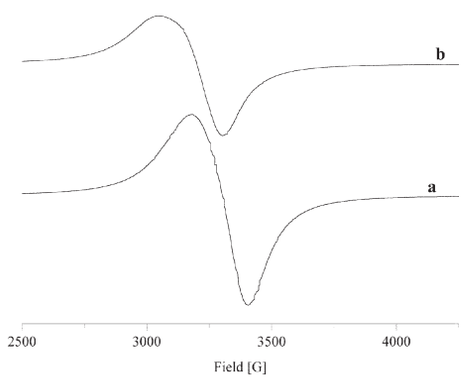

Fig. 3 Polycrystalline EPR spectra of the complex at the X band frequency at (a) 298 K and (b) 77 K.

To assess this possibility, the temperature dependence of the ESR was determined over the temperature range 100 to 340 K. The integrated ESR signal intensity as a function of temperature is shown in Fig. 4. The signal decreases nonlinearly by a factor of three as the temperature increases from 100 to 340 K.

If there is an exchange coupling between the two copper ions in adjacent chains, it is expected that the dimeric ground spin level will be $S = 0$ and the excited spin level will be $S = 1$. While the former level is diamagnetic and EPR-silent, the latter is paramagnetic. Thus, the observation of an ESR signal indicates that there must be some Boltzmann population in the $S = 1$ level. Qualitatively, the ESR signal intensity should be zero at very low temperatures, increase with increasing temperature, reach a maximum, and then decrease with a further increase in temperature.[36,37] By fitting the observed temperature dependence, it should be possible not only to prove that there is an exchange coupling present, but also to determine the extent of the coupling, that is to determine the exchange coupling parameter J.

Over fifty years ago, Bleaney and Bowers gave[38] the theoretical basis of antiferromagnetic exchange coupling in a dimeric copper complex, copper(II) acetate. The fraction of the population in the $S = 1$ state is given by:

$$P_{S=1} = 3e^{-J/kT}/[1 + 3e^{-J/kT}]$$

The difference in the population between adjacent magnetic field-split levels is:

$$P_{S=1}[1 - e^{-g\beta H/kT}]/3 \approx P_{S=1} g\beta H/3kT$$

Combining these equations, the predicted temperature dependence of the ESR signal intensity can be shown to be proportional to:

$$I \propto (1/T)[e^{-J/kT}/(1 + 3e^{-J/kT})]$$

We calculated the ESR signal intensity over the range $T = 100$ to 340 K using this equation, while varying J from 10–100 cm^{-1}. The minimum in the root mean square (rms) difference between the observed integrated signal and the predicted signal over all temperatures was sought. At 100 K, the predicted signal was normalized to the observed signal. The smallest rms difference was found for $J = 23 \pm 2$ cm^{-1}. The calculated and observed temperature dependence of the

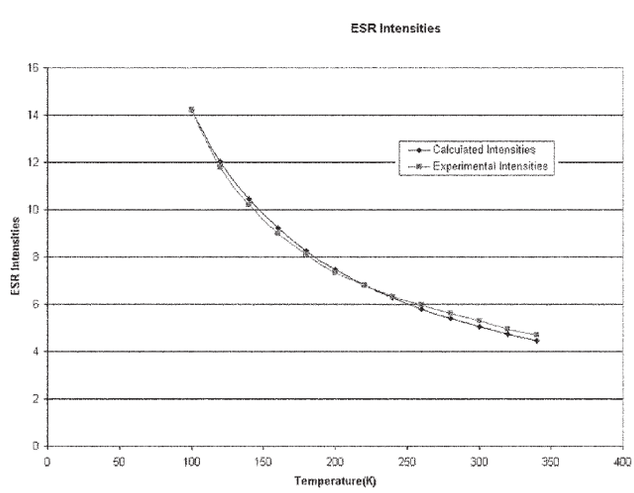

Fig. 4 Experimental and calculated temperature dependence of the ESR signal intensities of the copper complex.

ESR signal intensities are plotted in Fig. 4. The excellent match confirms our hypothesis that the copper ions are antiferromagnetically coupled in the $K[CuHL_2]\cdot H_2O$ solid. The small magnitude of the J coupling is reasonable for two coppers that are 4.248 Å distant, when compared to the Bleaney and Bowers value of $J = 260$ cm^{-1} found for two copper ions 2.64 Å apart in copper(II) acetate.[38]

Vibrational (IR and Raman) spectra of hpa and $K[CuHL_2]\cdot H_2O$

It is known that the hpa ligand forms a tetrameric structure in the solid state.[27] The tetramer structure of hpa (*cf.* Fig. 5) was computed using the HF/6-31G(d) approach only (because of convergence problems with the B3LYP method). The optimized bond distances and angles for the tetramer are in fairly good agreement with crystallographic data (*cf.* Table 2). The optimized H-bond lengths are slightly longer compared to the X-ray lengths: for $OH_{carboxyl}\cdots N$, computed = 2.990 Å, experimental = 2.755 Å and for $OH_{oximic}\cdots O_{carboxyl}$, computed = 2.799 Å, experimental = 2.686 Å.

In calculations of the complex (see Fig. 5), density functional theory (DFT/B3LYP) was used and the experimental Cu–N and Cu–O bond lengths held fixed at their experimental values (see Table 1).

The computed and experimental vibrational frequencies and assignments of the selected modes for hpa and $K[CuHL_2]\cdot H_2O$ are summarized in Table 3 (a full description of the vibrational spectra of the ligand and the complex are given in the ESI, Tables III and IV). The harmonic frequencies calculated by using the HF method were scaled only by a factor of 0.8953 for the 6-31G(d) basis set, as suggested by Scott and Radom.[39] Experimental (IR and Raman) spectra for the ligand and complex are shown in Figs. 6 and 7. Several absorptions of hpa and $K[CuHL_2]\cdot H_2O$ are interesting to consider since they change positions upon coordination. They are discussed below.

ν(OH), $\nu(CH_3)$ and $\delta(-H\cdots O^-)$. The IR spectra of hpa and $K[CuHL_2]\cdot H_2O$ exhibit broad smooth absorption bands centered at *ca.* 3200 and 3460 cm^{-1}, respectively. These are assigned to the strongly hydrogen-bonded OH of the ligand and to the free or weakly H-bonded hydrated and coordinated waters in the complex. The complexity of these bands may be attributed to several vibrational resonances between the ν(OH) fundamentals and various combinations or overtones. Thus, only a qualitative assignment of this band can be made. The broad hydroxyl group stretches overlap the weak CH_3 stretching IR bands. Therefore, the C–H stretching vibrations of both species have been characterized based on Raman spectra. For hpa, these modes generate one intense band at 2936 cm^{-1} with a shoulder at 2960 cm^{-1} and a weak band at 3034 cm^{-1}. Upon complexation, these vibrations are shifted to lower energy by ~12 cm^{-1}. The IR spectrum of the title complex exhibits a very weak band at 1763 cm^{-1}. This band is characteristic for oxime cis complexes and is assigned to the O–H bending frequency of the intramolecular hydrogen $O-H\cdots O^-$ bond.[22,40–42] Theoretical method predicts the presence of this vibration at 1864 cm^{-1}, as revealed by DFT and the calculated PED.

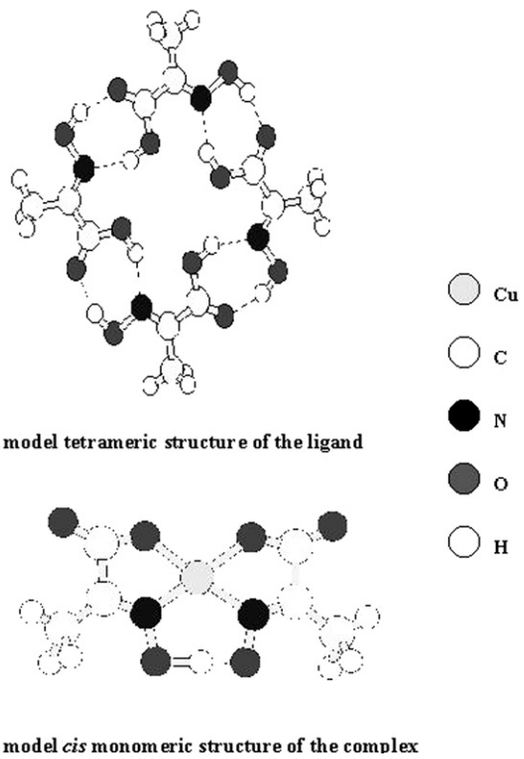

Fig. 5 Model structures of the ligand and the complex used in the calculations.

Table 2 Selected computed and experimental bond lengths (Å) and angles ° for hpa and $K[CuHL_2]\cdot H_2O$

Parameter	Hpa [HF/6-31G(d)]	Hpa (exptal[27])	$CuHL_2$ (B3LYP/Lanl2DZ)	$K[CuHL_2]\cdot H_2O$ (exptal)
C=N	1.256	1.274	1.307	1.276 1.287
N–O	1.343	1.380	1.385	1.352 1.360
C=O	1.198	1.211	1.261	1.233
C–O	1.306	1.314	1.329	1.287
C_{ox}–C_{car}	1.499	1.489	1.529	1.511
C_{ox}–C_{met}	1.501	1.484	1.497	1.489
C=N–O	115.4	112.8	119.9	120.5
O=C–O	124.5	124.8	126.7	124.1
N=C–C_{car}	115.6	115.6	113.1	111.7
N=C–C_{met}	127.2	125.8	124.3	125.3
O=C–C	120.5	120.4	119.4	119.3
O–C–C	115.1	114.7	113.8	116.3
C–C–C	117.2	118.6	122.6	122.3

ν_{as}(COO) and ν_s(COO). According to the theoretical results, the medium-strong infrared band at 1654 cm^{-1} can be attributed to the ν_{as}(COO) mode of the ligand, which mixes with the C=N stretching vibration. However, the Raman counterpart of this vibration, revealed by PED calculations (73%), is observed as a very strong band at 1656 cm^{-1}. The symmetric stretching modes of the hpa carboxyl group are observed at 1420 cm^{-1} (IR) and 1465 cm^{-1} (Raman). Both bands are very broad due to overlap with δCH_3 modes with similar frequencies. In the copper complex, the infrared COO absorption (asymmetric) is shifted to lower frequency at 1626 cm^{-1}, as expected for a coordinated carboxyl group. The considerable width of the experimental band is caused by a superposition of this mode with bending modes of water. In the Raman, the $\delta(H_2O)$ vibrations are not observable or very weak, thus the ν_{as}(COO) mode can be observed clearly at 1620 cm^{-1}. On the other hand, the symmetric COO vibration is shifted by *ca.* 60 cm^{-1} to lower energy after metal coordination and is observed at 1360 cm^{-1}.

The relationship between the frequency separation of the asymmetric and symmetric carboxyl vibrations and the structure of the coordinated COO group is well known.[43,44] An increase in $\nu_{as} - \nu_s$ of a complex relative to a ligand is connected with a more asymmetric structure of the carboxylate ion, caused by the more covalent character of the metal–carboxylate bond. In our case, $\nu_{as} - \nu_s$ of $K[CuHL_2]\cdot H_2O$ is greater than that of hpa by 30 cm^{-1}. Thus, the Cu–OOC bond is expected to be primarily covalent, which accounts for the

Table 3 Computed [with potential energy distribution (PED in %)] and experimental IR and Raman frequencies (in cm^{-1}) of selected modes for hpa and $K[CuHL_2]\cdot H_2O$

	Hpa [HF/6-31G(d)]		Hpa (exptal)		$CuHL_2$ (B3LYP/Lanl2DZ)		$K[CuHL_2]\cdot H_2O$ (exptal)	
Mode[a]	IR	Raman	IR	Raman	IR	Raman	IR	Raman
$\nu_{as}(CH_3)$	3009 (87)			3034	3176 (88)			3021
	2947 (97)		~2930	2960	3109 (99)		~2900	2956
$\nu_s(CH_3)$	2896 (83)			2936	3041 (88)			2924
$\delta_{as}(CH_3)$	1489(70)							
	1458 (81)		1468	1465	1506 (77)		~1400	1435
	1445 (58)				1498 (70)			
$\delta_s(CH_3)$	1399 (79)		1420	1377	1428 (89)			1381
$\rho(CH_3)$	974 (26)		989	986	1070 (60)		1082	–
$\nu_{as}(COO)$	1749 (65)	1775 (73)	1654	1656	1620 (78)		1626	1620
$\nu_s(COO)$	1426 (16)	1436 (28)	1420	1465	1337 (27)		1360	1364
$\beta(COO)$	828 (40)	–	817	–	869 (21)	–	870	–
$\omega(COO)$	745 (64)	–	761	–	740 (80)	–	731	–
$\nu(C{=}N)$	1777 (59)	1781 (53)	1695	1698	1649 (61)	1627 (14)	1683	1641
$\nu(NO)$	1102 (71)		1040	1054	1140 (42)(d) [b]		1142	1136
					1026 (13)(p)[b]		1020	–

[a] Modes are denoted as: ν stretching, δ scissoring, β bending in-plane, ω -wagging, ρ rocking. [b] The oximic group is (d) deprotonated or (p) protonated.

increase in complex stability. Similar behavior has been observed for the copper–α-alanine complex, where $\nu_{as} - \nu_s$ is 45 cm^{-1}.[45]

***β*(COO), *ω*(COO) and *ρ*(COO).** According to our calculations, the other COO vibrational modes of hpa, COO bending [*β*(COO)], COO wagging [*ω*(COO)] and COO rocking [*ρ*(COO)], contribute to the IR bands at 817(s), 761(m) and 705 (vs) cm^{-1}. The HF-predicted frequencies and intensities are in very good agreement with these IR results: 828 cm^{-1} [*β*(COO)], 745 cm^{-1} [*ω*(COO)] and 676 cm^{-1} [*ρ*(COO)]. As expected, coordination to the metal ion shifts the *β*(COO) mode (to 870 cm^{-1}; calculated as 869 cm^{-1} *via* B3LYP) and shifts the *ω*(COO) mode (to 731 cm^{-1}; calculated as 740 cm^{-1} *via* B3LYP). The COO rock is not observed. For the cis copper complex of α-alanine, the *β*(COO) mode is shifted to higher frequencies (+6 cm^{-1}) while the frequency of the *ω*(COO) vibration is down shifted by 17 cm^{-1}, as compared to the equivalent bands of α-alanine.[46]

***ν*(C=N) and *ν*(N–O).** From our normal coordinate analysis, the C=N ligand stretching mode shows a large contribution (59%) to the strong IR band at 1695 cm^{-1}, whereas the Raman band at 1698 cm^{-1} can be assigned to a mixed C=O and C=N vibration. The band positions of the oximic group in the metal complexes are dependent on the nature of the coordination. Based on the crystallographic data and spectroscopic literature,[25,41,42] the *ν*(C=N) mode of $K[CuHL_2]\cdot H_2O$ should be shifted to lower frequency compared to the hpa band and should be split as a result of the deprotonation of one of the oximic groups. According to the DFT calculation, the medium infrared band at 1683 cm^{-1} (1649 calculated) is assigned to *ν*(C=N) of the shorter protonated oximic bond, while the second weaker *ν*(C=N) of the oximato group is probably hidden under the other strong bands in the 1600–1680 cm^{-1} region. The B3LYP calculation did not predict the presence of the weaker *ν*(C=N) mode because the C=N lengths of the deprotonated and protonated oximic groups were computed to be closely similar.

In oximes, a strong N–O IR stretch is expected in the 870–1040 cm^{-1} range.[47] A strong, sharp IR band at 1040 cm^{-1} and a medium Raman band near 1054 cm^{-1} can be ascribed to the hpa *ν*(N–O) mode. In the copper complex, this vibration is shifted to higher frequency. This is strong support for ligand coordination through the nitrogen donors. The N–O stretching

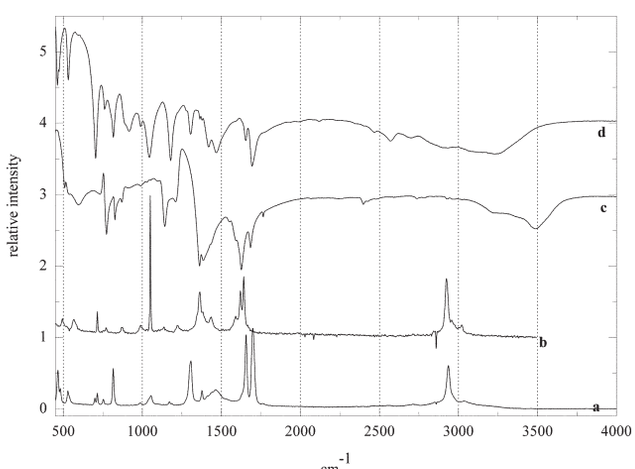

Fig. 6 Mid-IR and Raman spectra (4000–450 cm^{-1}) of hpa and $K[CuHL_2]\cdot H_2O$: (a) Raman spectrum of hpa, (b) Raman spectrum of the copper complex, (c) mid-IR spectrum of the copper complex, (d) mid-IR spectrum of hpa.

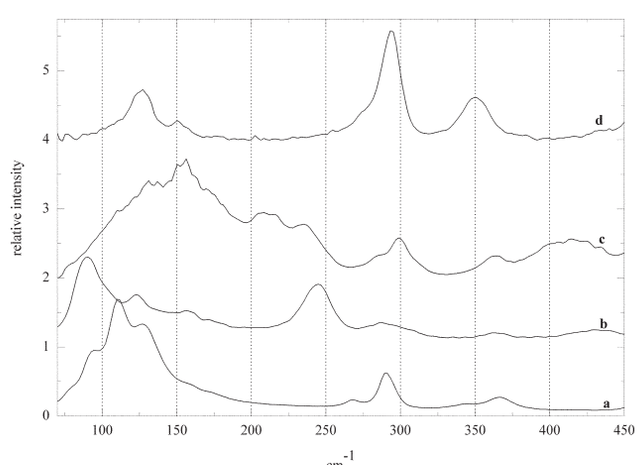

Fig. 7 Far-IR and Raman spectra (450–70 cm^{-1}) of hpa and $K[CuHL_2]\cdot H_2O$: (a) Raman spectrum of hpa, (b) Raman spectrum of the copper complex, (c) far-IR spectrum of the copper complex, (d) far-IR spectrum of hpa.

absorption in our copper complex is expected to be split due to the protonation of the oximic group. The protonated NO bond is elongated by removal of electron density from the bond and the absorption is thus expected at a lower frequency. Furthermore, NO^- is a more polar bond than NOH so its infrared absorption should be stronger. Hence, the oximato NO^- stretching vibration is observed at 1142 cm^{-1} in the IR. The analogous mode of the protonated NO group may be assigned to a very weak band at 1020 cm^{-1}. This assignment is consistent with studies on other metallo-oximes[22,23,48,49] as well as with our PED calculations. DFT calculations predict the NO stretching modes should appear as medium and weak IR bands at 1140 and 1026 cm^{-1}, respectively.

$\delta_{as}(CH_3)$, $\delta_s(CH_3)$ and $\rho(CH_3)$. Deformational vibrations of the methyl group are expected in the 1470–1300 and 1250–800 cm^{-1} ranges.[47] The asymmetric scissoring mode of the methyl group in hpa [$\delta_{as}(CH_3)$] has been assigned to the strong, broad IR band at 1468 cm^{-1} and the medium Raman band at 1465 cm^{-1} (computed: 1489, 1458, and 1445 cm^{-1}). The symmetric bending [$\delta_s(CH_3)$] and rocking [$\rho(CH_3)$] vibrations are observed at 1420 and 989 cm^{-1} in the hpa IR spectrum (1377 and 986 cm^{-1} in the Raman, respectively). The HF frequencies of these modes are in a good agreement with the experiment, being 1399 and 974 cm^{-1} for the symmetric scissoring and rocking modes. Upon chelation with copper, the $\delta_{as}(CH_3)$ and $\delta_s(CH_3)$ vibrations appear at 1435 and 1381 cm^{-1} in the Raman. The IR spectrum assignment is ambiguous due to the mixing of the $K[CuHL_2]\cdot H_2O$ vibrations with the strong absorption of the uncoordinated nitrate ion. The rocking mode is observed as a very weak intensity IR band at 1082 cm^{-1}. All of these assignments are supported by calculations, where absorptions at 1506, 1428 and 1070 cm^{-1} have been attributed to $\delta_{as}(CH_3)$, $\delta_s(CH_3)$ and $\rho(CH_3)$, respectively. In the α-alanine IR spectrum, the bands at 1455, 1362, and 1014 cm^{-1} are attributed to the same vibrations, respectively. Coordination to the copper ion shifts only the rocking CH_3 mode to much higher frequency (1220 cm^{-1}), while the asymmetric scissoring vibration is up-shifted by ~13 cm^{-1} and the absorption of the symmetric bend is unchanged.[50]

Cu–ligand vibrations. The frequency region below 500 cm^{-1} is particularly interesting since it can provide information on metal–ligand vibrations. The FT-IR and Raman spectra of hpa and $K[CuHL_2]\cdot H_2O$ in the 450–70 cm^{-1} range are shown in Fig. 7. The broad, medium intensity Raman band at 494 cm^{-1} is assigned to the asymmetric copper–nitrogen stretching vibration. This is supported by calculated PEDs, which predict this absorption at 506 cm^{-1}. Although the computed IR intensity is very weak, the Raman is of medium intensity, both as observed. The medium intensity IR band at 434 cm^{-1} is attributed to the in-phase (symmetric) stretching mode of the copper–oxygen bond. The B3LYP-predicted frequency (467 cm^{-1}) and intensity of this band are again in good agreement with experimental data. According to the PED, the asymmetric Cu–O and the symmetric Cu–N stretching vibrations have been attributed to the weak infrared and Raman band located at ~365 cm^{-1} (378 cm^{-1} calculated by using DFT). It should be mentioned that the corresponding asymmetric and symmetric Cu–N and Cu–O stretching modes in the cis copper–α-alanine complex were observed at 483, 411, 325, and 276 cm^{-1}, respectively.[46] This indicates that the strength of the metal–ligand bond in the complex studied here is stronger than in the α-alanine complex. Moreover, the presence of four active Cu–ligand stretching vibrations is consistent with symmetry arguments for the cis isomer (C_s point group). It can also be a vibrational criterion for the determination of cis and trans isomerism.[43,46] The DFT method predicts a strong Raman band at 245 cm^{-1} and a strong IR band at 152 cm^{-1} for the coupled stretching vibrations, $Cu–N_{(p)}$ with $Cu–O_{(d)}$ and $Cu–N_{(d)}$ with $Cu–O_{(p)}$, respectively.

Conclusions

An X-ray study of the copper complex of 2-hydroxyiminopropanoic acid has shown that it has cis bidentate square-planar geometry. This is similar to the solution geometry determined by Onindo and coworkers.[7] The copper ion is coordinated by carboxylic oxygens and the oximic nitrogens, creating two five-membered chelating rings. The structure is stabilized by an intramolecular H-bridge between the deprotonated and protonated oximic groups. The EPR data of polycrystalline $K[CuHL_2]\cdot H_2O$ indicates the presence of antiferromagnetically coupled copper ions, having a small exchange coupling parameter J (23 cm^{-1}). Such behavior is due to spin-spin interactions between pairs of paramagnetic metal ions located in the interplanar lattice sites (separated by 4.248 Å). The coordination of the carboxyl and oximic groups to the Cu(II) ion was confirmed by the experimental and theoretical vibration analysis. The observed splitting of the asymmetric and symmetric COO modes indicates the primarily covalent nature of the metal–carboxylate bond. Moreover, the formation of the cis isomer is determined by the presence of the characteristic weak band at 1763 cm^{-1}, assigned to the bending deformation of the intramolecular H-bond. This is also consistent with the presence of four Cu–ligand stretching vibrations, as expected by the complex's symmetry. Copper–hpa stretching frequencies are observed at higher energies than those of the corresponding copper–α-alanine complex. This indicates that the chelation of the copper ion by the oximic donor ligands strengthens the coordinate bonds in comparison to those in amino acid metal complexes.

References

1 G. E. Jackson and B. S. Nakani, *J. Chem. Soc., Dalton Trans.*, 1996, 1373.
2 R. W. Hartman, M. Hector, S. Haidar, P. B. Ehmer, W. Reichert and J. Jose, *J. Med. Chem.*, 2000, **43**, 4266.
3 E. H. Nardin, J. M. Calvo-Calle, G. A. Oliveira, R. S. Nussenzweig, M. Schneider, J. M. Tiercy, L. Loutan, D. Hochstrasser and K. Rose, *J. Immunol.*, 2001, **166**, 481.
4 S. X. Cai, Z.-L. Zhou, J.-C. Huang, E. R. Whittemore, Z. O. Egbuwoku, Y. Lü, J. E. Hawkinson, R. M. Woodward, E. Weber and J. F. W. Keana, *J. Med. Chem.*, 1996, **39**, 3248.
5 G. Petroianu, C. Roth, U. Beha, J. Fisher, W. Bergler and R. Rufer, *J. Appl. Toxicol.*, 2001, **21**, 7.
6 D. Mansuy, P. Battioni and J.-P. Battioni, *Eur. J. Biochem.*, 1998, **184**, 267.
7 C. O. Onindo, T. Y. Sliva, T. Kowalik-Jankowska, I. O. Fritsky, P. Buglyo, L. D. Pettit, H. Kozlowski and T. Kiss, *J. Chem. Soc., Dalton Trans.*, 1995, 3911.
8 T. Y. Sliva, A. Dobosz, L. Jerzykiewicz, A. Karaczyn, A. M. Moreeuw, J. Swiatek-Kozlowska, T. Glowiak and H. Kozlowski, *J. Chem. Soc., Dalton Trans.*, 1998, 1863.
9 T. Y. Sliva, T. Kowalik-Jankowska, V. M. Amirkhanov, T. Glowiak, C. O. Onindo, I. O. Fritskii and H. Kozlowski, *J. Inorg. Biochem.*, 1997, **65**, 287.
10 A. A. Mokhir, E. Gumienna-Kontecka, J. Swiatek-Kozlowska, E. G. Petkova, I. O. Fritskii, L. Jerzykiewicz, A. A. Kapshuk and T. Y. Sliva, *Inorg. Chim. Acta*, 2002, **329**, 113.
11 A. A. Dvorkin, Y. A. Simonov, V. V. Skopenko, I. O. Fritsky and R. D. Lampeka, *Dokl. Akad. Nauk SSSR*, 1990, **313**, 98.
12 A. A. Dvorkin, Y. A. Simonov, V. V. Skopenko, I. O. Fritsky and R. D. Lampeka, *Dokl. Akad. Nauk SSSR*, 1990, **310**, 87.
13 T. Y. Sliva, A. M. Duda, T. Glowiak, I. O. Fritsky, V. M. Amirkhanov, A. A. Mokhir and H. Kozlowski, *J. Chem. Soc., Dalton Trans.*, 1997, 273.
14 G. M. Sheldrick, *SHELXTL5*, Bruker-AXS, Madison, WI, USA, 1998.
15 C. Lee, W. Yang and R. G. Parr, *Phys. Rev. B*, 1988, **37**, 785.
16 A. D. Becke, *J. Chem. Phys.*, 1993, **98**, 5648.

17 P. J. Hay and W. R. Wadt, *J. Chem. Phys.*, 1985, **82**, 299.
18 P. J. Hay and W. R. Wadt, *J. Chem. Phys.*, 1985, **82**, 270.
19 M. J. Frisch, G. W. Trucks, H. B. Schlegel, G. E. Scuseria, M. A. Robb, J. R. Cheeseman, V. G. Zakrzewski, J. A. Montgomery, Jr., R. E. Stratmann, J. C. Burant, S. Dapprich, J. M. Millam, A. D. Daniels, K. N. Kudin, M. C. Strain, O. Farkas, J. Tomasi, V. Barone, M. Cossi, R. Cammi, B. Mennucci, C. Pomelli, C. Adamo, S. Clifford, J. Ochterski, G. A. Petersson, P. Y. Ayala, Q. Cui, K. Morokuma, D. K. Malick, A. D. Rabuck, K. Raghavachari, J. B. Foresman, J. Cioslowski, J. V. Ortiz, B. B. Stefanov, G. Liu, A. Liashenko, P. Piskorz, I. Komaromi, R. Gomperts, R. L. Martin, D. J. Fox, T. Keith, M. A. Al-Laham, C. Y. Peng, A. Nanayakkara, C. Gonzalez, M. Challacombe, P. M. W. Gill, B. G. Johnson, W. Chen, M. W. Wong, J. L. Andres, M. Head-Gordon, E. S. Replogle and J. A. Pople, *GAUSSIAN 98 (Revision A.6)*, Gaussian, Inc., Pittsburgh, PA, 1998.
20 M. H. Jamroz, *Vibrational Energy Distribution Analysis: Veda 3.0 Program*, Drug Institute, Warsaw, Poland, 2000.
21 J. Hanss, A. Beckmann and H.-J. Kruger, *Eur. J. Inorg. Chem.*, 1999, 163.
22 L. F. Szczepura, J. G. Muller, C. A. Bessel, R. F. See, T. S. Janik, M. R. Churchill and K. J. Takeuchi, *Inorg. Chem.*, 1992, **31**, 859.
23 A. Chakravorty, *Coord. Chem. Rev.*, 1974, **13**, 1.
24 V. Manivannan, B. K. Dirghangi, C. K. Pal and A. Chakravorty, *Inorg. Chem.*, 1997, **36**, 1526.
25 V. Y. Kukushkin, T. Nishioka, D. Tudela, K. Isobe and I. Kinoshita, *Inorg. Chem.*, 1997, **36**, 6157.
26 S. Kawata, S. Kitagawa, H. Machida, T. Nakamoto, M. Kondo, M. Katada, K. Kikuchi and I. Ikemoto, *Inorg. Chim. Acta*, 1995, **229**, 211.
27 J. K. Maurin, *Acta Crystallogr., Sect. C*, 1995, **51**, 2111.
28 C. K. Pal, S. Chattopadhyay, C. Sinha and A. Chakravorty, *Inorg. Chem.*, 1994, **33**, 6140.
29 J. D. Martin, K. A. Abboud and K.-H. Dahmen, *Inorg. Chem.*, 1998, **37**, 5811.
30 C. L. Perrin and J. B. Nielson, *Annu. Rev. Phys. Chem.*, 1997, **48**, 511.
31 M. E. Keeney and K. Osseo-Asare, *Coord. Chem. Rev.*, 1984, **59**, 141.
32 A. S. El-Tabl and T. I. Kashar, *Pol. J. Chem.*, 1998, **72**, 519.
33 P. Lemoine, B. Viossat, G. Morgant, F. T. Greenaway, A. Tomas, N.-H. Dung and J. R. J. Sorenson, *J. Inorg. Biochem.*, 2002, **89**, 18.
34 K. Kurdziel, T. Glowiak and J. Jezierska, *Polyhedron*, 2002, **21**, 1857.
35 C. Karunakaran, K. R. J. Thomas, A. Shunmugasundaram and R. Murugesan, *Mol. Phys.*, 2002, **100**, 287.
36 B. C. Guha, *Proc. Roy. Soc. London, Ser. A*, 1951, **206**, 353.
37 C. J. Ballhausen, *Introduction to Ligand Field Theory*, McGraw-Hill Co., New York, 1962, p. 271.
38 B. Bleany and K. D. Bowers, *Proc. Roy. Soc. London, Ser. A*, 1952, **214**, 451.
39 A. P. Scott and L. Radom, *J. Phys. Chem.*, 1996, **100**, 16 502.
40 J. E. Caton and C. V. Banks, *Inorg. Chem.*, 1967, **6**, 1670.
41 N. Yoshida, A. Furusaki and M. Fujimoto, *J. Chem. Soc., Dalton Trans.*, 1991, 453.
42 A. Gül and Ö. Bekâroğlu, *J. Chem. Soc., Dalton Trans.*, 1983, 2537.
43 K. Nakamoto, *Infrared and Raman Spectra of Inorganic and Coordination Compounds*, 5th edn., John Wiley & Sons, Inc., New York, 1997, Part B.
44 D. T. Sawyer and P. J. Paulsen, *J. Am. Chem. Soc.*, 1959, **81**, 816.
45 K. Nakamoto, Y. Morimoto and A. E. Martell, *J. Am. Chem. Soc.*, 1961, **83**, 4528.
46 A. W. Herlinger, S. L. Wenhold and T. V. Long, *J. Am. Chem. Soc.*, 1970, **92**, 6474.
47 D. Lin-Vien, N. B. Colthup, W. G. Fateley and J. G. Grasselli, *The Handbook of Infrared and Raman Characteristic Frequencies of Organic Molecules*, Academic Press, Inc., San Diego, 1991.
48 A. L. Crumbliss and P. L. Gaus, *Inorg. Chem.*, 1975, **14**, 486.
49 V. Alexander, *Inorg. Chim. Acta*, 1993, **204**, 109.
50 G. C. Percy and H. S. Stenton, *J. Chem. Soc., Dalton Trans.*, 1976, 2429.